Magnetic properties of (misch metal, Nd)-Fe-B melt-spun magnets

R. Li, R. X. Shang, J. F. Xiong, D. Liu, H. Kuang, W. L. Zuo, T. Y. Zhao, J. R. Sun, and B. G. Shen

---

Articles you may be interested in

Micromagnetic simulation of the influence of grain boundary on cerium substituted Nd-Fe-B magnets
AIP Advances **7**, 056201 (2016); 10.1063/1.4972803

Structure and properties of sintered MM–Fe–B magnets
AIP Advances **7**, 056215 (2017); 10.1063/1.4973603

Coercivity of Nd-Fe-B hot-deformed magnets produced by the spark plasma sintering method
AIP Advances **7**, 056205 (2016); 10.1063/1.4973438

Magnetic properties of Sm-Fe-N bulk magnets produced from Cu-plated Sm-Fe-N powder
AIP Advances **7**, 056204 (2016); 10.1063/1.4973396

The magnetic properties of $MMCo_5$ (MM=Mischmetal) nanoflakes prepared by multistep (three steps) surfactant-assisted ball milling
AIP Advances **7**, 056203 (2016); 10.1063/1.4973395

Magnetic properties of $Nd(Fe_{1-x}Co_x)_{10.5}M_{1.5}$ (M=Mo and V) and their nitrides
AIP Advances **7**, 056202 (2016); 10.1063/1.4973207

Magnetic properties of (misch metal, Nd)-Fe-B melt-spun magnets

R. Li,[1,2] R. X. Shang,[1,2] J. F. Xiong,[1,2] D. Liu,[1,2] H. Kuang,[1,2] W. L. Zuo,[1,2] T. Y. Zhao,[1,2] J. R. Sun,[1,2] and B. G. Shen[1,2,a]

[1]*State Key Laboratory of Magnetism, Institute of Physics, Chinese Academy of Sciences, Beijing 100190, People's Republic of China*
[2]*University of Chinese Academy of Sciences, Beijing 100049, People's Republic of China*

The effect of replacing Nd with misch metal (MM) on magnetic properties and thermal stability has been investigated on melt-spun $(Nd_{1-x}MM_x)_{13.5}Fe_{79.5}B_7$ ribbons by varying x from 0 to 1. All of the alloys studied crystallize in the tetragonal 2:14:1 structure with single hard magnetic phase. Curie temperature (T_c), coercivity (H_{cj}), remanence magnetization (B_r) and maximum energy product ($(BH)_{max}$) all decrease with MM content. The melt-spun $MM_{13.5}Fe_{79.5}B$ ribbons with high ratio of La and Ce exhibit high magnetic properties of $H_{cj} = 8.2$ kOe and $(BH)_{max} = 10.3$ MGOe at room temperature. MM substitution also significantly strengthens the temperature stability of coercivity. The coercivities of the samples with x = 0.2 and even 0.4 exhibit large values close to that of $Nd_{13.5}Fe_{79.5}B_7$ ribbons above 400 K. © *2017 Author(s). All article content, except where otherwise noted, is licensed under a Creative Commons Attribution (CC BY) license (http://creativecommons.org/licenses/by/4.0/).* [http://dx.doi.org/10.1063/1.4973846]

I. INTRODUCTION

With the increasing demand for NdFeB permanent magnets and the extensive use of Nd in natural rare-earth resources, the rising price of Nd induces cost pressures on the NdFeB material industry. Developing low-cost rare-earth permanent magnet becomes particularly important. For this purpose, the issue on substituting Nd with the most abundant and inexpensive light rare-earth metal La or Ce has drawn continuing interests.[1–8] This work aims to obtain $R_2Fe_{14}B$ based hard magnets using misch metal (MM) alloys with high La and Ce contents (unseparated rare-earth mixtures: La-Ce-Pr-Nd alloy). Although both saturation magnetization and magnetocrystalline anisotropy of $La_2Fe_{14}B$ and $Ce_2Fe_{14}B$ are inferior to that of $Nd_2Fe_{14}B$,[9] MM-substituted permanent magnets are potential alternative and economical materials with intermediate magnetic properties filling the gap between ferrites and NdFeB magnets.[10,11] Unfortunately, sintered or die-upset magnets with high La or Ce ratios usually exhibit very low coercivities because of their seriously deteriorated microstructure.[11,12] By contrast, completely or excessively replaced magnets prepared by the melt-spun method can achieve promising magnetic properties. For example, Ko *et al.*[13] reported that melt-spun $MM_{12}Fe_{82}B_6$ alloy exhibited a coercivity of 5.6 kOe and a maximum energy product of 8.9 MGOe, Yamasaki *et al.*[3] recorded $H_{cj} = 9.4$ kOe and $(BH)_{max} = 8.1$ MGOe in a $MM_{16}Fe_{75}B_9$ alloy. The MM used in these studies contains approximately 30 wt.% La, 50 wt.% Ce and 20 wt.% Pr-Nd, and $MM_2Fe_{14}B$ can theoretically achieve an increased maximum potential energy product of 10 MGOe as isotropic magnet.[14] Further effort, such as optimizing alloy composition or enhancing orientation, can be exerted to improve the magnetic properties of these kinds of low-cost magnets.

In addition, melt-spun magnetic powder used to make isotropic bonded or injection molded magnets should constantly provide sufficient high magnetic properties at or above 400 K. Given the

[a]Author to whom correspondence should be addressed. Electronic mail: shenbg@iphy.ac.cn

low Curie temperature (T_c = 424 K) of $Ce_2Fe_{14}B$,[9] excessive substitution of Nd with MM degrades the intrinsic magnetic properties of RFeB magnets at elevated temperature. Most investigations only reported the room temperature magnetic properties of MMFeB magnets, but few studies have been performed on the effects of MM on the temperature stability of magnetic properties. In this work, we prepare $(Nd_{1-x}MM_x)_{13.5}Fe_{79.5}B_7$ ribbons via the melt-spun method. The Curie temperature and magnetic properties above room temperature are investigated with varying MM content. High magnetic properties of H_{cj} = 8.2 kOe and $(BH)_{max}$ = 10.3 MGOe are obtained in $MM_{13.5}Fe_{79.5}B_7$ alloy. Replacing Nd with MM affords the magnets with enhanced temperature stability of coercivity. The ribbons with x = 0.2 and even 0.4 exhibit the same coercivity as that of NdFeB above 400 K.

II. EXPERIMENT

Ingots having nominal compositions of $(Nd_{1-x}MM_x)_{13.5}Fe_{79.5}B_7$ (x = 0, 0.2, 0.4, 0.6, 0.8, 1) are fabricated by arc melting under an argon atmosphere of 99.9% Fe, 99.9% Nd, 99.7% MM and 97% ferroboron (FeB). The MM alloy consists of 28.3 wt.% La, 50.5 wt.% Ce, 5.2 wt.% Pr, 15.7 wt.% Nd and 0.3 wt.% others (approximately to the same ratio of rare earth elements found in natural ore). Each ingot is remelted at least five times to ensure composition homogeneity. The melt-spun ribbons are produced by induction melting the ingot in quartz tubes with a 0.5 mm diameter bottom orifice under 1/2 atm of high purity Ar gas. The melted ingot is then ejected at a 60 torr overpressure onto a rotating copper wheel. The optimum tangential wheel velocity ranges from 20 m/s to 25 m/s. Typical ribbons possess a thickness and width of approximately 30-50 μm and 2-3 mm, respectively. The ribbons are then crushed to powders, and these powders are examined with X-ray diffraction (XRD) using Cu Kα radiation. Curie temperatures for all samples are determined by the magnetization of polycrystalline samples as a function of temperature with a vibrating sample magnetometer (VSM) in a static field of 500 Oe. The hysteresis loops of all samples are measured in a Physical Property Measurement System (PPMS) made by Quantum Design Inc. in a magnetic field of up to 70 kOe and temperatures up to 650 K.

III. RESULTS AND DISCUSSION

Fig.1 displays the XRD patterns of melt-spun ribbons with optimal magnetic properties in $(Nd_{1-x}MM_x)_{13.5}Fe_{79.5}B_7$ (x = 0, 0.2, 0.4, 0.6, 0.8, 1) alloys. The results show line characteristics of the tetragonal $Nd_2Fe_{14}B$ structure in all cases and no additional phases (rare earth oxides, RFe_2 or α-Fe). These findings confirm that all samples contain a single-phase with MM replacement. According to Scherer's formula, the average grain sizes are estimated within the range of 30-50 nm.
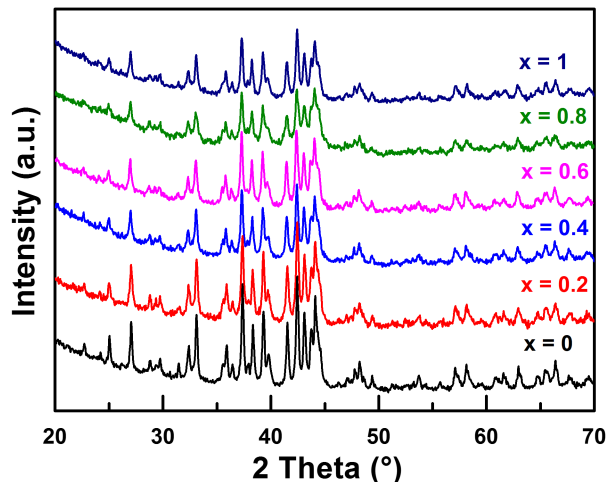

FIG. 1. The X-ray diffraction patterns for $(Nd_{1-x}MM_x)_{13.5}Fe_{79.5}B_7$ ribbons (x = 0, 0.2, 0.4, 0.6, 0.8, 1).

Diffraction peaks are slightly broadened, and some peaks are obviously weakened with increasing MM concentration. A reasonable explanation is that amorphous phases and metastable phases at intergranular interface in these ribbons are easily formed and increased because of different phase equilibria in the La-Fe-B, Ce-Fe-B, Pr-Fe-B and Nd-Fe-B systems.[7]

The variation of intrinsic coercivity (H_{cj}), remanence (B_r) and maximum energy product (($BH)_{max}$) at room temperature and the Curie temperature (T_c) of all samples are summarized in Table I. These data include the corresponding mass proportions of La and Ce and Pr-Nd in MM metal. The room temperature magnetic properties (H_{cj}, B_r, and ($BH)_{max}$) and T_c all show linear decreases with MM content. The decrease in magnetic properties is attributed to the drop in intrinsic magnetic properties, because the intrinsic magnetic properties of $La_2Fe_{14}B$ and $Ce_2Fe_{14}B$ are lower than that of $Pr_2Fe_{14}B$ and $Nd_2Fe_{14}B$. The decrease in Curie temperature is ascribed to T_c of $Ce_2Fe_{14}B$ being lower than that of $La_2Fe_{14}B$, $Pr_2Fe_{14}B$ or $Nd_2Fe_{14}B$. This result also suggests that MM atoms enter into the 2:14:1 phase. According to previous studies, paramagnetic or soft magnetic phase (LaO or CeO, RFe_2, RFe_4B_4, or Fe-rich phases, and unclear grain boundaries) easily exist in sintered or die-upset magnets because of the strong tendency of oxidation of La or Ce or the instability of $La_2Fe_{14}B$ phase or the diffusion of multiple rare-earth elements at high temperature.[11,15–18] Consequently, sintered or die-upset magnets containing high La or Ce content with poor microstructure tend to obtain very low coercivities or even lose their hard magnetic properties. However, large coercivities could be achieved in nanocrystalline magnets fabricated by melt-spun method with enhanced microstructure. This effect is achieved because the unfavorable factors mentioned above can be greatly suppressed by the non-equilibrium process of fast cooling. For example, in high La- and Ce-addition magnets, such as $MM_2Fe_{14}B$ in this work, the stoichiometric $MM_{12}Fe_{82}B_6$ melt-spun alloy reportedly exhibits a coercivity of 5.6 kOe.[13] Similar to the method of increasing the rare earth or boron content to enlarge coercivity, rich-MM and rich-B based MMFeB magnets obtained higher coercivities, and the maximum values reported reach approximately 25% of magnetocrystalline anisotropy field (H_a = 4 T[14]), such as H_{cj} = 9.4 kOe for $MM_{16}Fe_{75}B_9$[3] and H_{cj} = 10 kOe for $MM_{22}Fe_{70}B_8$.[19] To avoid low maximum energy product in rich-MM and rich-B based magnets because of the increase in non-magnetic phases, the melt-spun ribbons designed in this work with a nominal composition of $MM_{13.5}Fe_{79.5}B_7$ achieve an acceptable intrinsic coercivity and a high maximum energy product (H_{cj}=8.2 kOe and ($BH)_{max}$=10.3 MGOe).

The remanence and intrinsic coercivity of melt-spun $(Nd_{1-x}MM_x)_{13.5}Fe_{79.5}B_7$ (x = 0, 0.2, 0.4, 0.6, 0.8, 1) as a function of temperature from 300 K to 500 K are displayed in Figs. 2(a) and (b). Their temperature coefficients for remanence (α) and coercivity (β) are listed in Table I. Fig. 2(a) shows that the reduction trend of B_r gradually enlarges with the increasing MM content and the remanences of the samples with x=0.8 and 1 drop rapidly as temperature approaches their Curie temperature. These findings indicate that the temperature stability of remanence worsens by MM addition and α decreases from -0.13 %/K to -0.22 %/K. Because α is inversely related to the Curie temperature T_c,[20] Ce addition in magnets, which results in the low T_c, is the reason for the decrease in the temperature stability of remanence. On the contrary, in Fig. 2(b), H_{cj} show opposite reduction trends with the varying content of MM and β increases from -0.42 %/K to -0.33 %/K. This result suggests that replacing Nd with MM is good for enhancing the temperature stability of coercivity.

TABLE I. The content of La, Ce, and Pr-Nd in the total rare earth and the room temperature magnetic properties and the Curie temperatures and the temperature coefficients for remanence (α) and coercivity (β) of $(Nd_{1-x}MM_x)_{13.5}Fe_{79.5}B_7$ ribbons with x=0, 0.2, 0.4, 0.6, 0.8, 1.

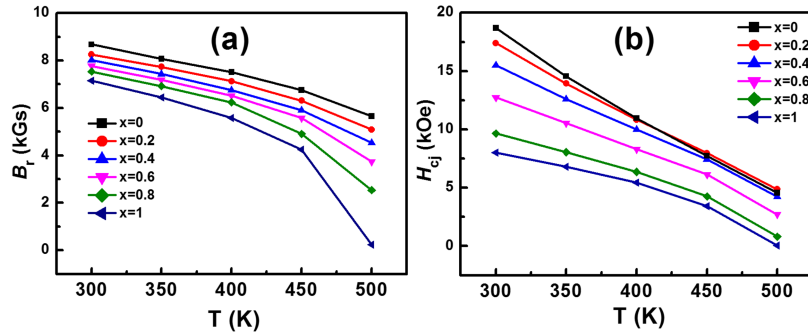| Samples	La (wt.%)	Ce (wt.%)	Pr-Nd (wt.%)	H_{cj} (kOe)	B_r (kGs)	$(BH)_{max}$ (MGOe)	T_c (K)	α (%/K)	β (%/K)
0	0	0	100.0	18.7	8.7	16.0	592	-0.13	-0.42
0.2	5.7	10.1	84.2	17.4	8.4	15.1	579	-0.14	-0.38
0.4	11.3	20.2	68.5	15.5	8.0	13.7	563	-0.15	-0.38
0.6	17.0	30.3	52.7	12.5	7.8	12.6	541	-0.16	-0.35
0.8	22.6	40.4	37.0	10.0	7.5	11.5	525	-0.17	-0.33
1	28.3	50.5	21.2	8.2	7.2	10.3	503	-0.22	-0.33

FIG. 2.   (a) B_r and (b) H_{cj} of $(Nd_{1-x}MM_x)_{13.5}Fe_{79.5}B_7$ (x = 0, 0.2, 0.4, 0.6, 0.8, 1) from 300 to 500 K.

Interestingly, the intrinsic coercivity of the sample with x = 0.2 does not decrease considerably before ~400 K compared with that of $Nd_{13.5}Fe_{79.5}B_7$, and it is even slightly larger than that of $Nd_{13.5}Fe_{79.5}B_7$ after ~400 K. Moreover, the intrinsic coercivity above 450 K for the sample with x = 0.4 attains a large value close to $Nd_{13.5}Fe_{79.5}B_7$. The rare earth sites in $R_2Fe_{14}B$ have different crystalline electric field parameters and Fe coordination numbers, which results in different temperature dependence of the magnetocrystalline anisotropy.[9,21] H_a of $Pr_2Fe_{14}B$ and $Nd_2Fe_{14}B$ arises from the large R moment with an orbital angular moment L≠0, which leads to large crystal-field splitting. However, their H_a show strong temperature dependence and a monotonic decline with increasing temperature. The L=0 compounds $La_2Fe_{14}B$ and $Ce_2Fe_{14}B$ have low H_a which are completely contributed by the iron sublattice, but their H_a show weak temperature dependence. Moreover, the temperature dependence of H_a above room temperature is anomalous for $La_2Fe_{14}B$ and it presents a trend of increasing first and then decreasing. For a solid solution of $R_2Fe_{14}B$, temperature dependence of magnetocrystalline anisotropy is expected to follow a rule of mixtures. Thus, the inclusion of La and Ce in solid solution with Pr and Nd in the $R_2Fe_{14}B$ phase should enhance the temperature dependence of H_a and accordingly improve the temperature stability of coercivity. This effect is present in the $(RNd)_2Fe_{14}B$ magnets where improved temperature stability of coercivity has been successfully developed.[22–24] In spite of replacing by La or Ce with low anisotropy field, $(Nd_{1-x}MM_x)_{13.5}Fe_{79.5}B_7$ (84.2 wt.% Pr-Nd) and $(Nd_{1-x}MM_x)_{13.5}Fe_{79.5}B_7$ (68.5 wt.% Pr-Nd) ribbons in this work obtain large coercivities at high temperature.

According to the magnetic hardening mechanism, besides on magnetocrystalline anisotropy field, the intrinsic coercivity strongly depends on the microstructure of magnet, which can be phenomenologically expressed by the following micromagnetic equation:[25]

$$\frac{H_{cj}}{M_s} = \alpha_k \alpha_{ex} \alpha_\varphi \frac{H_a}{M_s} - N_{eff} M_s$$

Where α_k, α_{ex}, α_φ, and N_{eff} are so called microstructural parameters and related to non-ideal microstructure of the real magnets. The parameter α_k reflects the locally reduction of crystal anisotropy of the inhomogeneous surface regions, α_{ex} describes the effect of exchange coupling between the neighboring grain, α_φ is related to the grain orientation distribution (generally equal to 0.5) and N_{eff} is the effective demagnetization factor due to the enhanced stray fields at the edges and corners of the grains. The values $H_a(T)$ of $La_2Fe_{14}B$, $Ce_2Fe_{14}B$, $Pr_2Fe_{14}B$ and $Nd_2Fe_{14}B$ phases are collected from the previous work[9] and then are used to calculate $H_a(T)$ for each sample according to the percentage of La, Ce, Pr and Nd. By linear fit of H_{cj}/M_s vs H_a/M_s plot (the fitting curves of the samples with x=0, 0.6 and 1 are shown in Fig.3), $\alpha_k \alpha_{ex}$ and N_{eff} for all samples increase from 0.55 and 0.09 to 0.64 and 0.28 with MM increasing, respectively. It is known that Curie temperature is controlled by Fe(3d)-Fe(3d) and R(4f)-Fe(3d) exchange and the exchange constant can be evaluated by the Curie temperature. The decrease in Curie temperature with MM content proves a smaller exchange constant between atoms in the unit cell and it indicates a weaker intergranular exchange coupling. Hence, the increase of $\alpha_k \alpha_{ex}$ can be attributed to the weak exchange coupling between the
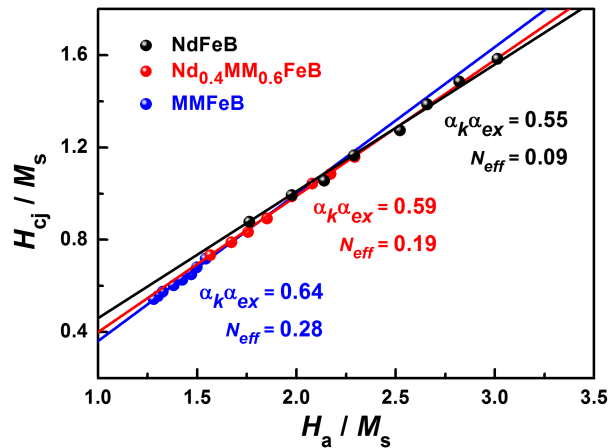
FIG. 3. H_{cj}/M_s values plotted against H_a/M_s values for the samples with x=0, 0.6 and 1.

grains, and the increase of N_{eff} is owing to the increase of local stray fields at the edges and corners of the grains because of the weakened smoothing effect of the exchange interaction.[25]

IV. CONCLUSION

In this work, melt-spun $(Nd_{1-x}MM_x)_{13.5}Fe_{79.5}B_7$ ribbons with single hard magnet phase are successfully prepared. With the increase of MM content, magnetic properties, such as H_{cj}, B_r, and $(BH)_{max}$, all drop because of the decrease in intrinsic magnetic properties by La and Ce replacement. High percentage of La-Ce melt-spun $MM_{13.5}Fe_{79.5}B_7$ ribbons exhibit a high room temperature performance with $H_{cj} = 8.2$ kOe and $(BH)_{max} = 10.3$ MGOe. The temperature stability of coercivity is strengthened through MM substitution and the replaced magnets with x = 0.2 and even 0.4 maintain large coercivities above 400 K. Using MM can significantly reduce the cost of rare-earth permanent magnets with acceptable performance.

[1] O. Gutfleisch, M. A. Willard, E. Brück, C. H. Chen, S. G. Sankar, and J. P. Liu, Adv. Mater. **23**, 821–842 (2011).
[2] A. K. Pathak, M. Khan, K. A. Gschneidner, Jr., R. W. McCallum, L. Zhou, K. Sun, K. W. Dennis, C. Zhou, F. E. Pinkerton, M. J. Kramer, and V. K. Pecharsky, Adv. Mater. **27**, 2663–2667 (2015).
[3] J. Yamasaki, H. Soeda, M. Yanagida, K. Mohri, N. Teshima, O. Kohmoto, T. Yoneyama, and N. Yamaguchi, IEEE. Trans. Magn. **22**(5), (1986).
[4] W. Z. Tang, S. Z. Zhou, and R. Wang, J. Appl. Phys. **65**, 3142 (1989).
[5] D. Li and Y. Bogatin, J. Appl. Phys. **69**, 5515 (1991).
[6] W. C. Chang, S. H. Wu, B. M. Ma, and C. O. Bounds, J. Magn. Magn. Mater. **167**, 65–70 (1997).
[7] J. F. Herbst, M. S. Meyer, and F. E. Pinkerton, J. Appl. Phys. **111**, 07A718 (2012).
[8] Z. B. Li, B. G. Shen, M. Zhang, F. X. Hu, and J. R. Sun, J. Alloys. Comp. **628**, 352–328 (2015).
[9] J. F. Herbst, Rev. Mod. Phys. **63**, 4 (1991).
[10] R. Skomski, J. Phys.: Condens. Matter. **15**, R841–R896 (2003).
[11] E. Niu, Z. A. Chen, G. A. Chen, Y. G. Zhao, J. Zhang, X. L. Rao, B. P. Hu, and Z. X. Wang, J. Appl. Phys. **115**, 113912 (2014).
[12] K. Y. Ko, S. Yoon, and J. G. Booth, J. Magn. Magn. Mater. **176**, 313–320 (1997).
[13] K. Y. Ko, J. G. Booth, H. J. Al-Kanani, and H. Y. Lee, J. Mag. **1**, 82–85 (1996).
[14] M. Jurczyk, J. Mag. Mag. Mater. **73**, 199–204 (1988).
[15] H. H. Stadelmaier, N. C. Liu, and N. A. Elmasry, Mater. Lett. **3**, 3 (1985).
[16] M. Umadevi and K. P. Gupta, J. Less-Common. Meta. **159**, 13–21 (1990).
[17] S. L. Huang, H. B. Feng, M. G. Zhu, A. H. Li, Y. Zhang, and W. Li, AIP. Adv. **4**, 107127 (2014).
[18] C. J. Yan, S. Guo, R. J. Chen, D. Lee, and A. R. Yan, IEEE. Trans. Magn. **50**(11), (2014).

[19] O. Popov, V. Skumryev, and M. Mikhov, J. Magn. Magn. Mater. **71**, L7–L9 (1987).

[20] X. G. Cui, M. Yan, T. Y. Ma, W. Luo, and S. J. Tu, Sci. Sinter. **41**, 91–99 (2009).

[21] S. Hirosawa, Y. Matsuura, H. Yamamoto, S. Fujimura, M. Sagawa, and H. Yamauchi, J. Appl. Phys. **59**, 873 (1986).

[22] C. J. Yan, S. Guo, L. Chen, R. J. Chen, J. Liu, D. Lee, and A. R. Yan, IEEE. Trans. Magn. **52**(5) (2016).

[23] Z. M. Chen, Y. K. Lim, and D. Brown, IEEE. Trans. Magn. **51**(11), (2015).

[24] W. Tang, Y. Q. Wu, K. W. Dennis, N. T. Oster, M. J. Kramer, I. E. Anderson, and R. W. McCallum, J. Appl. Phys. **109**, 07A704 (2011).

[25] D. Goll and H. Kronmüller, Sci. Nat. **87**, 423–438 (2000).